International Journal of Engineering, Mathematical and Physical Sciences
ISSN: 2517-9934
Vol:7, No:8, 2013

Statistical Description of Wave Interactions in 1D Defect Turbulence

Yusuke Uchiyama and Hidetoshi Konno

Abstract—We have investigated statistical properties of the defect turbulence in 1D CGLE wherein many body interaction is involved between local depressing wave (LDW) and local standing wave (LSW). It is shown that the counting number fluctuation of LDW is subject to the sub-Poisson statistics (SUBP). The physical origin of the SUBP can be ascribed to pair extinction of LDWs based on the master equation approach. It is also shown that the probability density function (pdf) of inter-LDW distance can be identified by the hyper gamma distribution. Assuming a superstatistics of the exponential distribution (Poisson configuration), a plausible explanation is given. It is shown further that the pdf of amplitude of LDW has a fat-tail. The underlying mechanism of its fluctuation is examined by introducing a generalized fractional Poisson configuration.

Keywords—sub-Poisson statistics, hyper gamma distribution, fractional Poisson configuration.

I. Introduction

THE complex Ginzburg-Landau equation (CGLE) is one of the most studied equations in nonlinear physics [1]. It describes various phenomena such as Rayleigh-Bénard convection in thermal fluid systems [3]–[5], propagation of chemical waves in reaction-diffusion systems [6]–[8], optical signal transmission in dissipative media [9]–[11], and so on. The CGLE is a typical normal form equation near local bifurcation points in non-equilibrium opening systems [12]. Actually, various phenomena occurring in non-equilibrium systems have been studied based on the features of the CGLE in the past decades.

Particularly, complex spatiotemporal dynamics of the CGLE such as the defect turbulence has been attracting many physicists' attentions [2]. Defect is defined as a singular point where phase slips. It is known that the CGLE has particularly various different types of defects in any spatial dimensions: hole, spiral wave and vortex line, which are observed in one, two and three dimensional systems. Especially in 1D system, hole has analytical form known as the "Bekki-Nozaki (BN) hole" [13].

Chaté extensively investigates spatiotemporal dynamics of the 1D CGLE [14]. He classifies some different types of spatiotemporal dynamics in the phase diagram of normalized linear dispersion and nonlinear dissipation coefficients. Howard and Hecke introduce a phenomenological coupled map lattice model in focussing on neighbor interaction of phases [15], [16] to mimic the defect turbulence. They suggest that holes interplaying in self-disordered background can cause the defect turbulence. Sherratt and Smith demonstrate a transition process from stable plane wave to the defect turbulence under zero-linear dispersion limit [17]. In their simulations, one can see a splitting process of BN-hole like local depressing waves (LDW) and local standing waves (LSW), and after that this process leads to the defect turbulence. It seems that the above waves are regarded as one of the key events in the defect turbulence.

On statistical analysis of the CGLE, Sakaguchi studies some statistical properties of "soliton turbulence" under zero-nonlinear dispersion limit [18]. His analysis is performed under the spatiotemporal dynamics with many body interaction among solitons with radiations. That is, soliton-soliton interaction with radiations plays the key role in the soliton turbulence, since waveform of soliton is involved in the CGLE under the nonlinear Schrödinger equation with a weak dissipation. We have been focusing on some statistical properties of the defect turbulence. In our previous work [19], we have reported some probability distributions of physical quantities from a viewpoint of mathematical statistics. The detailed physical descriptions of their properties of the defect turbulence with discussions on the mechanisms have not given.

Here the present paper, by focusing on LDW, reports on the stochastic dynamical laws involved in the fluctuations of (i) counting number of LDW, (ii) inter-LDW distance and (iii) amplitude of LDW. In section II, the method of our numerical simulation for the defect turbulence in the 1D CGLE is explained briefly. Section III presents the stochastic dynamical laws describing the mechanisms of the statistical properties of the defect turbulence: (a) the counting number fluctuation of LDW is analyzed with the use of a master equation; (b) the inter-LDW distance is quantified as a superstatistics of Poisson configuration; and (c) the pdf of amplitude of LDW is modeled by a fractional generalization of Poisson configuration. Section IV is devoted to conclusions.

II. Numerical Simulation

The 1D CGLE is described in the form [1]:

$$\frac{\partial A}{\partial t} = A + (1+ic_1)\frac{\partial^2 A}{\partial x^2} - (1+ic_2)|A|^2 A, \qquad (1)$$

where A is a complex variable, c_1 and c_2 are real parameters called as linear and nonlinear dispersion coefficients, respectively. Numerical simulation of Eq. (1) is performed under the periodic boundary condition. Figure 1 shows a stationary state, when a weak random perturbation is adopted as an initial condition. In Fig. 1 (a), waveforms of some LDWs and LSWs are recognized. Phase is depicted in an extended phase

Y. Uchiyama is with the Department of Risk Engineering, Faculty of Information and Systems, University of Tsukuba, Tsukuba, Ibaraki 305-8573, Japan e-mail: r1230160@risk.tsukuba.ac.jp.

H. Konno is with the Department of Risk Engineering, Faculty of Information and Systems, University of Tsukuba, Tsukuba, Ibaraki 305-8573, Japan e-mail: konno.hidetoshi.fu@u.tsukuba.ac.jp.

space in Fig. 1 to exhibit discontinuity of phase. To solve Eq. (1), the fourth order Runge-Kutta scheme for time and the second order central differential scheme for space are utilized. System size L is fixed with $L = 500$, the corresponding space resolution and time step are $\Delta x = 0.5$ and $\Delta t = 0.01$, respectively. The linear and the nonlinear dispersion coefficient are fixed with $c_1 = 1.5$ and $c_2 = -1.2$, which correspond to the defect turbulence regime [14].

The numerical simulation under boundary and the initial condition gives a spatiotemporal profile of A in Figs. 2: (a) black region indicates amplitude near zero and pale brown region indicates LSW; (b) one can find some discontinuities of phase, which correspond to LDWs near zero amplitude. In Fig. 3 (a snapshot of Fig. 2), a disordered configuration of LDWs and LSWs is clearly observed. From careful observation of the dynamical behavior of LDW and LSW, they can be regarded as local elementary excitations in the defect turbulence.

On account of numerous observations in our simulations, statistical properties of the defect turbulence associated with many body interaction between LDW and LSW will be displayed in the next sections.

III. Statistical Analysis

In our statistical analysis, LDW is naively defined as a local depression from the background ($|A| = 0.8$), and LSW is identified by a local maximum of amplitude. Then the statistical properties of LDW like counting number, interdistance and amplitude are analyzed. Specifically, these fluctuations are evaluated in each time step of the simulation in the whole space. The procedure of the statistical analysis will be explained in the next subsections.

A. The counting number fluctuation of LDW

Figure 4 shows the probability distribution of the the counting number of LDW, which is identified well by the binomial distribution:

$$B(p,k) = {}_nC_k p^k (1-p)^{n-k}, \tag{2}$$

where n is the maximum counting number in the whole space, p is probability that LDW is generated and k is the counting number of LDW, respectively. The parameters in Eq. (2) are estimated by the mean $\langle k \rangle$ and the variance σ_k^2 as n = 41 and p = 0.2. To classify statistics, the Fano factor (FF) is available:

$$FF = \frac{\sigma_k^2}{\langle k \rangle}. \tag{3}$$

The FF takes a value less than 1 ($FF = 0.8$). This means that the counting number fluctuation of LDW is subject to the sub-Poisson (SUBP) statistics. In the case of the squeezed state of light [20], the SUBP nature is due to the photon antibunting. From analogy with light, a kind of "LDW bunching state" may be expected. In this subsection, we will try to find the origin of the sub-Poisson nature of the fluctuation in the case of the defect turbulence.

To elucidate the underlying mechanism of the appearance of the SUBP statistics, let us write down elementary interaction schemes of the local waves in the defect turbulence after careful observation of Fig. 2: (i) two LDWs collide and turn into one LSW, (ii) two LSWs merge after collision, (iii) one LDW and one LSW connect and turn into one LDW reversibly, (iv) one LDW turns into one LSW, (v) one LDW and one LSW emerge from background. These interaction schemes are described below:

$$2X \xrightarrow{k_1'} Y, \tag{4a}$$

$$2Y \xrightarrow{k_2'} Y, \tag{4b}$$

$$X + Y \underset{k_4'}{\overset{k_3'}{\rightleftarrows}} X, \tag{4c}$$

$$X \xrightarrow{k_5'} Y, \tag{4d}$$

$$0 \xrightarrow{k_6'} X, \tag{4e}$$

$$0 \xrightarrow{k_7'} Y, \tag{4f}$$

where X and Y are counting number of LDW or of LSW, and $k_i'(1 \le i \le 7)$ are the rates of reactions.

Although it is desirable to analyze the full reaction which involves the detailed interactions between X and Y, one can catch the main feature only from the knowledge of X, by using adiabatic approximation about Y, which is described by

$$2X \xrightarrow{k_1} 0, \tag{5a}$$

$$0 \underset{k_3}{\overset{k_2}{\rightleftarrows}} X, \tag{5b}$$

where $k_i(1 \le i \le 3)$ are the rates of reactions which correspond to the simplified elementary processes: (i) pair extinction process (Eq. (5a)) and (ii) creation process (left-pointing arrow in Eq. (5b)), which are the key mechanisms to give rise to the SUBP statistics in a "soliton turbulence" [21]. Thus we can say that an appropriate balance of these processes is the origin of a kind of "bunching state" in the many body interaction of the local waves.

The above processes lead to the transition probability (TP) for X in the system as

$$\begin{aligned} W(X, \Delta X, t) = {} & k_1 X(X-1)\delta_{\Delta X,-2} \\ & + k_2 \delta_{\Delta X,1} + k_3 X \delta_{\Delta X,-1}, \end{aligned} \tag{6}$$

where ΔX is transition rate of X and $\delta_{i,j}$ is the Kronecker's delta. From the above TP, the corresponding master equation is immediately derived as:

$$\begin{aligned} \frac{\mathrm{d}}{\mathrm{d}t} P(X,t) = {} & k_1(X+2)(X+1)P(X+2,t) \\ & + k_2 P(X-1,t) + k_3(X+1)P(X+1,t) \\ & - [k_1 X(X-1) + k_2 + k_3 X] P(X,t), \end{aligned} \tag{7}$$

where $P(X,t)$ is the time-dependent probability distribution for X.

Although the governing equation of $P(X,t)$ is obtained, in general, it is hard to solve analytically the master equation. Therefore, in many cases, the master equation is solved numerically [22]. On the other hand, in order to evaluate the moments from $P(X,t)$, the Poisson representation can be

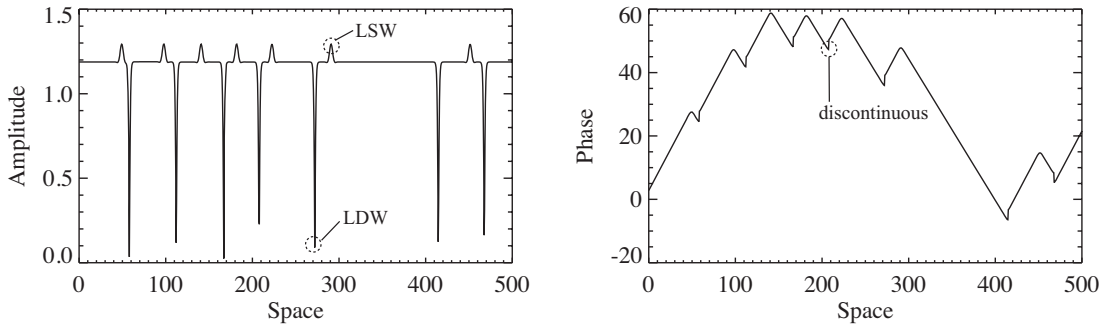

Fig. 1. A stationary configuration of LDWs and LSWs is obtained from a simulation with a certain parameter set described in Ref. [14]. In amplitude profile, LDWs and LSWs are recognized. Discontinuity and local maximum of phase correspond to LDW and LSW, respectively. Amplitude of the NB-hole reaches zero. On the other hand, amplitude of LDW does can not. Note that the phase is depicted in an extended phase space to exhibit phase discontinuities clearly.

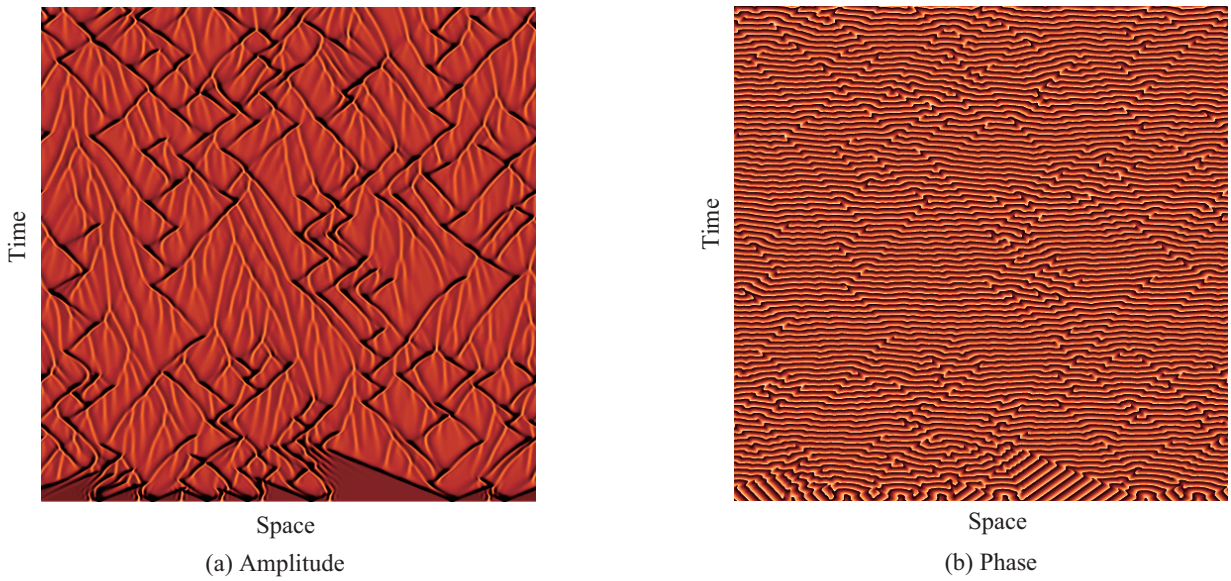

Fig. 2. Spatiotemporal dynamics of Eq. (1): (a) amplitude $|A|$ and (b) phase $\arg A$. In both (a) and (b), horizontal and vertical directions correspond to space and time, respectively. In our simulation, the parameters in Eq. (1) are fixed with $c_1 = 1.5$ and $c_2 = -1.2$. In the amplitude image (a), black region and pale brown region indicate LDW and LSW, respectively.

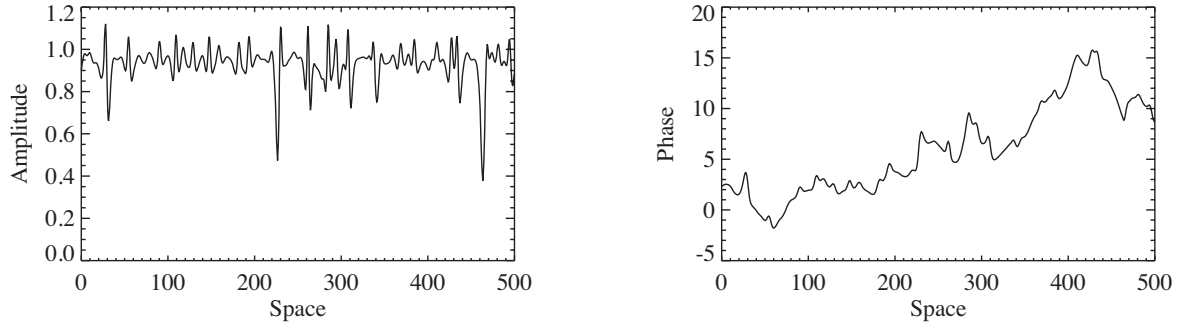

(a) Amplitude (b) Phase

Fig. 3. Snapshot of the defect turbulence: (a) amplitude $|A|$ and (b) phase $\arg A$. In the amplitude image (a), one can observe chaotic interplay between LDW and LSW. Also, disordered structure can be seen in the extended phase space (b).

utilized [23]. The definition of the complex Poisson representation is described by

$$P(X,t) = \int_C \frac{\mathrm{e}^{-\xi}\xi^X}{X!} f(\xi,t)\mathrm{d}\xi, \tag{8}$$

where ξ is a complex variable and C is a integral contour in complex plane. From Eq. (7) and Eq. (8), the governing equation of $f(\xi,t)$ is obtained in the form:

$$\frac{\partial}{\partial t}f(\xi,t) = -\frac{\partial^2}{\partial \xi^2}[(k_1\xi^2)f(\xi,t)] - \frac{\partial}{\partial \xi}[(-2k_1\xi^2 + k_2 + k_3\xi)f(\xi,t)]. \tag{9}$$

Note that the negative diffusion in right-hand side of Eq. (9) leads to unstable probability distribution. In spite of the above notification, the stationary distribution of Eq. (9) can be formally obtained. As steady state, namely the condition that $\partial_t f(\xi,t) = 0$, the stationary distribution $f_s(\xi)$ is immediately obtained as:

$$f_s(\xi) = \xi^{-(2+a_2)}\exp\left(2\xi + \frac{a_1 L^2}{\xi}\right), \tag{10}$$

where $a_1 = k_2/k_1L^2$, $a_2 = k_3/k_1$ and L is the system size. By the representation of $f_s(\xi)$ in Eq. (10) with rescaled variable $\xi = \eta L$, the r-th moment $\langle \xi^r \rangle$ is described by

$$\langle \xi^r \rangle = \frac{\oint \xi^r f_s(\xi)\mathrm{d}\xi}{\oint f_s(\xi)\mathrm{d}\xi}, \tag{11}$$

where the integration with respect to ξ can be carried out along a closed contour encircling the origin of complex plane. From Eq. (11), arbitrary order moment can be calculated exactly. As a result, the analytical form of the $\langle \xi^r \rangle$ is obtained as

$$\langle \xi^r \rangle = \left(L\sqrt{\frac{a_1}{2}}\right)^r \frac{I_{r-(a_2+1)}(2L\sqrt{2a_1})}{I_{a_2+1}(2V\sqrt{2a_1})}, \tag{12}$$

where $I_d(\cdot)$ is the d-th order modified Bessel function [24]. From below relations: $\langle X \rangle = \langle \xi \rangle$ and $\sigma_X^2 = \langle \xi^2 \rangle - \langle \xi \rangle^2 + \langle \xi \rangle$ [23], FF is asymptotically evaluated as follows:

$$FF = \frac{\frac{3}{4}L\sqrt{a_1/2} + O(1)}{L\sqrt{a_1/2} + O(1)} \approx \frac{3}{4}. \tag{13}$$

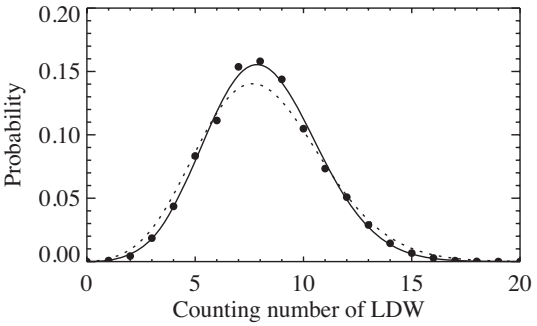

Fig. 4. The probability distribution of the counting number of LDW (black circles) is identified by the binomial distribution (solid line) better than the Poisson distribution (dashed line). The FF of counting number of LDW and the corresponding binomial distribution are '0.8', though that of the Poisson distribution is '1'. This is that the counting number fluctuation of LDW is subject to the SUBP statistics.

The FF value gives a good approximation for our result of simulation (see Fig. 4). This means that our simplified elementary processes are essential to catch the underlying mechanism of counting number fluctuation of LDW.

B. The fluctuation of inter-LDW distance

Here, we try to analyze the fluctuation of inter-LDW distance by reasonable extension of the Poisson configuration. Figure 5 shows that the pdf of the fluctuation of inter-LDW distance has two dominant peaks. One is the delta function type, which is located around '5.5'. The other is the hill-type function like the gamma distribution, where the peak is located near '25'. The former peak is originated from the LDW bunching state as is mentioned before. After eliminating the contribution of the delta function type peak, we can identify the latter contribution (see Fig. 6) by the hyper gamma distribution $f_{HG}(y;\alpha,\beta,\gamma)$ as

$$f_{HG}(y;\alpha,\beta,\gamma) = \frac{\beta^{\gamma/\alpha}}{\Gamma(\gamma/\alpha)} y^{\gamma-1}\exp(-\beta y^\alpha), \tag{14}$$

where, y is a random variable with respect to inter-LDW distance, α, β and γ are real parameters, $\Gamma(\cdot)$ is the gamma

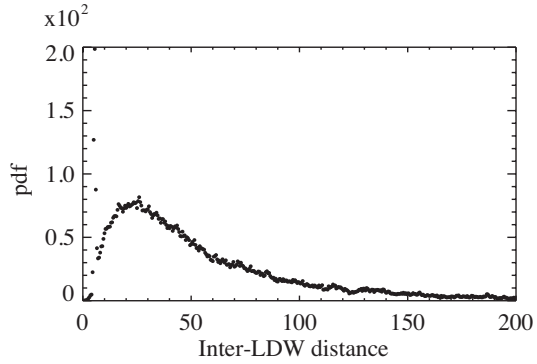

Fig. 5. The pdf of inter-LDW distance has two dominant peaks. One is the delta function-type, which is located around "5.5". The other is the hill-type function like the gamma distribution, where the peak is located near '25'.

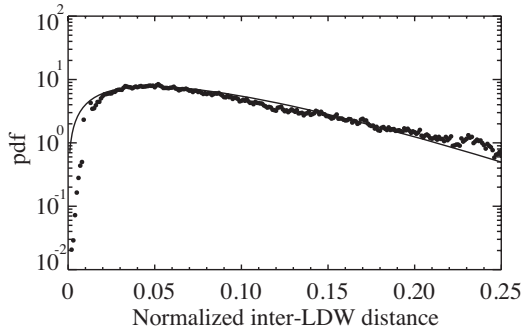

Fig. 6. The pdf of inter-LDW distance without contribution of the delta-function like peak is well identified by the hyper gamma distribution. To simplify calculation, horizontal axis is normalized by the system size L. Black circles represent the simulation result and solid line is the hyper gamma distribution with the parameter set: $\alpha = 1.18$, $\beta = 24.2$ and $\gamma = 1.79$.

function [25]. The estimated parameters are $\alpha = 1.18$, $\beta = 24.2$ and $\gamma = 1.79$. Note that the horizontal axis in Fig. 6 is normalized for the sake of brevity.

Among the many possible physical explanations which give rise to the hyper gamma distribution, we adopt a superstatistical approach [26] with the Poisson configuration. After eliminating the effect of the LDW bunching state which causes the SUBP statistics, the emerging event of LDW may be governed by the Poisson statistics with a slowly fluctuating parameter. Since inter-LDW distance is subject to the exponential distribution, the resulting pdf of inter-LDW distance $p(y)$ under its fluctuated parameter is described by

$$p(y) = \int_0^\infty p(y|\lambda) g(\lambda) \mathrm{d}\lambda, \tag{15}$$

where $p(y|\lambda) = \lambda \mathrm{e}^{-\lambda y}$ and $g(\lambda)$ is the pdf of positive parameter λ. To satisfy the condition that $p(y)$ equals the hyper gamma distribution, the specific form of $g(\lambda)$ is determined by

$$D_\lambda \left[D_\lambda^\alpha - \frac{1}{\alpha\beta} D_\lambda \lambda + \frac{2-\gamma}{\alpha\beta} \right] g(\lambda) = 0, \tag{16}$$

where α, β and γ are the same parameters in Eq. (14), D_λ is a linear operator defined by

$$D_\lambda = \frac{\mathrm{d}}{\mathrm{d}\lambda} + \frac{1}{\lambda}. \tag{17}$$

Although the specific form of $g(\lambda)$ can be obtained from Eq. (16), the α-th order operator D_λ^α, since α is a non-integer value in our case, makes Eq. (16) difficult to solve analytically. However, in special case that $\alpha = 1$, Eq. (16) leads to the hypergeometric differential equation, and thus $g(\lambda)$ is analytically obtained in terms of the hypergeometric function [24]. In this case, the corresponding pdf leads to the gamma distribution.

C. The amplitude fluctuation of LDW

Now, consider the amplitude fluctuation of LDW. Before carrying out stochastic analysis, in order to deal with the amplitude fluctuation of LDW as a stochastic process with respect to one parameter, let us make notice of the constraint on the periodic boundary condition $A(0,t) = A(L,t)$, namely a circular configuration.

Figure 7 shows the pdf of the amplitude fluctuation of LDW with normalized axes. The pdf has (i) a fat-tail and (ii) a cut-off amplitude. Neglecting the truncated structure, we try to construct a mathematical model of the amplitude distribution of LDW. The LDW bunching state suggests the existence of strong spatial correlation. To describe the spatial correlation, a fractional derivative is introduced. Then amplitude of LDW in the circular configuration is modeled as a generalized fractional Poisson configuration (FPC) [27] with fractional space derivative and fractional power backward shift operator:

$$\begin{aligned} &\frac{\mathrm{d}^\nu}{\mathrm{d}z^\nu} p(l,z) = -\theta^\mu (1-B)^\mu p(l,z), \\ &p(l,0) = \delta_{l,0}, \end{aligned} \tag{18}$$

where l and z are random variables with respect to amplitude and space configuration, respectively, $p(l,z)$ is a pdf of l and z, $\mu, \nu \in (0,1]$, θ is a real parameter, B is the so-called backward shift operator defined by $Bp(l,z) = p(l-1,z)$ and $\delta_{i,j}$ is the Kronecker's delta. Note that when $\mu = 1$ and $\nu = 1$, Eq. (18) leads to the ordinary Poisson configuration. The solution of Eq. (18) is immediately obtained by the generating function method as

$$p(l,z) = \frac{(-1)^l}{l!} \sum_{r=0}^\infty \frac{(-\theta^\mu z^\nu)^r}{\Gamma(\nu r + 1)} \frac{\Gamma(\mu r + 1)}{\Gamma(\mu r + 1 - l)}, \tag{19}$$

where $\Gamma(\cdot)$ is the gamma function.

Figure 7 shows that $p(l,z)$ in Eq. (19) with a certain parameter set ($\mu = 0.605$, $\nu = 0.72$ and $\lambda = 0.05$) is comparable to our result of simulation: the theoretical FPC agrees quite well with the amplitude-pdf. This result indicates that bursting event which has high value of amplitude can be caused by the spatial correlation. Without spatial correlation ($\nu = 1$), the relaxation of the pdf becomes the exponential decay, and thus, relative frequency of bursting event is very rare. However, the actual pdf involves the fat-tail, that is, appearance of LDW burst is not rare. Therefore, our formulation may be useful for analyzing physical nature of bursting events.

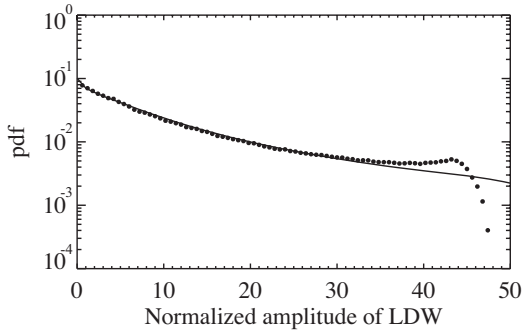

Fig. 7. Amplitude of LDW is normalized by system size, L. The pdf has (i) a fat-tail and (ii) a cut-off amplitude. The theoretical FPC (solid line) with $\mu = 0.605$, $\nu = 0.72$ and $\lambda = 0.05$ agrees quite well with the pdf of our simulation (black circles) except the truncation over higher values of the amplitude of LDW.

IV. Conclusion

The statistical properties of the defect turbulence in the 1D CGLE is studied in this paper. The fluctuating quantities (the counting number of LDW, inter-LDW distance and amplitude of LDW) are quantified from the viewpoint of statistical mathematics. Then the physical mechanisms associated with these quantities are studied theoretically: (i) The counting number fluctuation of LDW is modeled by the master equation based on LDW and LSW interaction schemes. It is shown that this fluctuation is subject to the sub-Poisson statistics, and thus, the role of a kind of "LDW bunching state" is elucidated. (ii) The pdf of inter-LDW distance has two different components: (a) the nearest neighbor delta function and (b) the hyper gamma distribution. The former is the contribution from the LDW bunching state. The latter is identified by a superstatistics of which the parameter of the exponential distribution is non-uniformly distributed. (iii) To model the amplitude fluctuation of LDW, FPC [27] with fractional order space derivative and fractional power backward shift operator is examined. Consequently, the FPC accords quite well with the result of our simulation except the point of the truncated tail. This accordance implies a new possibility for analyzing physical nature of burst emergence by a FPC type formulation.

Acknowledgment

This work is partially supported by Grant-in-Aid for JSPS Fellows No. 25.374.

References

[1] I. S. Aranson and L. Kramer, Rev. Mod. Phys. **74**, 99 (2002).
[2] J. Lega, Physica D, **152-153**, 269 (2001).
[3] H. W. Müller, M. Tveitereid and S. Trainoff, Phys. Rev. E **48**, 263 (1993).
[4] M. van Hecke and W. van Saarloos, Phys. Rev. E **55**, R1259 (1997).
[5] Y. Liu and R. E. Ecke, Phys. Rev. E **59**, 4091 (1999).
[6] A. T. Winfree, Science **175**, 634 (1972).
[7] Y. Kuramoto, *Chemical Oscillations, Waves and Turbulence*, Springer Verlag, 1984.
[8] A. S. Mikhailov and K. Showalter, Phys. Rep. **425**, 79 (2006).
[9] Y. Kodama and A. Hasegawa, Opt. Lett. **17**, 31 (1992).
[10] L. F. Mollenauer, J. P. Gordon and S. G. Evangelides, Opt. Lett. **17**, 1575 (1992).
[11] C. Paté, L. Gagnon and P. A. Bélanger, Opt. Commun. **74**, 228 (1989).
[12] J. D. Gibbon and M. J. Mcguiness, Proc. R. Soc. Lond. A, **377**, 185 (1981).
[13] N. Nozaki and N. Bekki, J. Phys. Soc. Jpn. **53**, 1581 (1984).
[14] H. Chaté, Nonlinearity **7**, 185 (1994).
[15] M. van Hecke and M. Howard, Phys. Rev. Lett. **86**, 2018 (2001).
[16] M. Howard and M. van Hecke, Phys. Rev. E **68**, 026213 (2003).
[17] J. Sherratt and M. J. Smith, Physica D **241**, 1671 (2012).
[18] H. Sakaguchi, Phys. Rev. E **76**, 017205 (2007).
[19] Y. Uchiyama and H. Konno, Proceedings of the 20th Australian Institute of Physics Congress, New South Wales, Australia, 9-13 December 2012.
[20] H. Haken, Light: Vol. 1: Waves, Photons, Atoms, North Holland, 1981.
[21] H. Konno and P. S. Lomdahl, J. Phys. Soc. Jpn. **69**, 1629 (2000).
[22] D. T. Gillespie, J. Phys. Chem. **81**, 2340 (1977), Y. Cao, D. T. Gillespie and L. R. Petzold, J. Phys. Chem. **122**, 014116 (2005), D. T. Gillespie, Annu. Rev. Phys. Chem. **58**, 35 (2007).
[23] C. Gardiner, Stochastic Methods: A Handbook for the Natural and Social Sciences, Springer Verlag, 2009.
[24] M. Abramowitz and I. A. Stegun, Handbook of Mathematical Functions: With Formulas, Graphs, and Mathematical Tables, Dover, 1972.
[25] E. Suzuki, Met. and Geophys. **18**, 103 (1967).
[26] C. Beck, Physica A **306**, 189 (2002).
[27] E. Orsinger and F. Polito, Stat. and Prob. Lett. **82**, 852 (2012).